

# DYNAMIC THREE-DIMENSIONAL RIGID BODY INTERACTION WITH HIGHLY DEFORMABLE SOLIDS, A MATERIAL POINT APPROACH

Robert Bird<sup>1\*</sup>, Giuliano Pretti<sup>1</sup>, William M. Coombs<sup>1</sup>, Charles E. Augarde<sup>1</sup>, Yaseen U. Sharif<sup>2</sup>, Michael J. Brown<sup>2</sup>, Gareth Carter<sup>3</sup>, Catriona Macdonald<sup>3</sup>, Kirstin Johnson<sup>3</sup>

<sup>1</sup>Department of Engineering, Durham University, Durham, England, UK.  
robert.e.bird@durham.ac.uk

<sup>2</sup>School of Science and Engineering, University of Dundee, Dundee, Scotland, UK.

<sup>3</sup>British Geological Survey, Edinburgh, Scotland, UK.

**Abstract.** The ability to model rigid body interaction with highly deformable solids is a very useful tool in geoen지니어ing, including the modelling of drag anchors on seabeds and seabed ploughing [7, 1]. However, these simulations entail several numerical challenges, such as modelling frictional contact, and incorporating inertia forces for analyses whose simulated time is considerable. Here the implicit Generalised Interpolation Material Point Method (GIMPM) is adopted to model the highly deformable solid, whilst a rigid body is used to model the significantly stiffer engineering object, such as an anchor. The whole system is integrated in time with the Newmark method with interaction between the two bodies occurring through a normal penalty contact and a penalty enforced Coulomb stick-slip friction law.

**Key words:** *Material Point Method; 3-dimensional; contact; rigid body*

## 1 Introduction

Understanding the penetration potential of an anchor is important for buried offshore infrastructure, such as power transmission cables for offshore renewable energy installations. However, modelling the penetration of an anchor into the seabed is challenging due to non-linear processes (large deformation, plasticity, contact) that must be taken into account. In this work an implicit GIMPM [4] is used to model the soil, whilst the anchor is represented by a discretised rigid body. The interaction between the bodies is achieved using a penalty contact [3]. An implicit analysis is used since it facilitates larger time increments compared to explicit approaches, particularly important with a refined discretisation. This paper outlines the key ingredients required to model anchor penetration using the material point method.

## 2 GIMP formulation with rigid body contact

For this approach an updated Lagrangian framework is adopted to model a system undergoing large deformations, [5, 4]. The weak statement for a material with domain,  $\Omega$  and boundary  $\partial\Omega$ , interacting with a rigid body,  $\Omega_R$ , with boundary,  $\partial\Omega_R$ , via the contact surface  $\partial\Omega_C \subset \partial\Omega_R$  is

$$\underbrace{\int_{\Phi_t(\Omega)} (\nabla_x \eta)_{ij} \sigma_{ij} dV + \int_{\Phi_t(\Omega)} \rho \eta_i \ddot{u}_i dV - \int_{\Phi_t(\Omega)} \eta_i b_i dV}_{\text{deformable body}} + \underbrace{\int_{\Phi_t^R(\Omega_R)} \rho_R \zeta_i \dot{w}_i dV - \int_{\Phi_t^R(\Omega_R)} \eta_i g_i dV}_{\text{rigid body}} + \int_{\Phi_t^R(\partial\Omega_C)} (\zeta_i - \eta_i) f_i dS = 0 \quad (1)$$

where the component in the last row is the contact between the two bodies. For the deformable body,  $\phi_t$  is its motion,  $\eta$  the test function,  $\sigma_{ij}$  is Cauchy stress,  $u_i$  are the displacements with acceleration  $\ddot{u}_i$ ,  $\nabla_x$  is the gradient operator in the updated coordinate system (denoted by the lower case  $x$ ),  $b_i$  is the body force.  $\phi_t^R$  is the motion of the rigid body,  $w_i$  and  $\ddot{w}_i$  are its displacement and acceleration,  $\zeta$  is the test function, and  $g_i$  is the body force. Here the rigid body is considered to be the *main* contact surface whilst the deformable body is the *secondary*, the interaction between the two therefore is integrated over the contact surface of the rigid body  $\phi_t^R(\partial\Omega_C)$  with  $f_i$  being the normal and frictional forces imparted from the deformable body onto the rigid body modelled using the penalty method [2].

The domain corresponding to the deformable body,  $\Omega$ , is discretised by a number of GIMP material points on a regular hexahedral background grid, with the GIMP basis used to link the material points  $p$  to the vertices of the background grid  $v$ , [4]. The GIMP basis functions and associated derivatives take the matrix forms  $[S_{vp}]$  and  $[\nabla S_{vp}]$ . The rigid body domain is discretised by tetrahedral elements  $K$  to form the mesh  $\mathcal{T}$ , with flat triangular elements  $\partial K$  discretising the contact boundary  $\partial\mathcal{T}_c$ . Linear basis functions are used for the tetrahedral and triangular elements of the rigid body and have the respective matrix forms  $[M]$  and  $[\hat{M}]$ . With these definitions, the discretised form of (1) is

$$\begin{aligned} \{R\} = & \mathbf{A} \left( [\nabla_x S_{vp}]^T \{\sigma_p\} V_p + \rho [S_{vp}]^T \{\ddot{u}_p\} - [S_{vp}]^T \{b\} \right) V_p \\ & + \sum_{K \in \mathcal{T}} \int_K \rho [C]^T [M]^T \{\ddot{w}_h\} dV - \sum_{K \in \mathcal{T}} \int_K \rho [C]^T [M]^T \{g\} dV + \{R_c\}, \end{aligned} \quad (2)$$

where  $\{R_c\}$  is the contact residual, described in the next section,  $[C]^T$  is a condensation matrix that ensures no relative movement between rigid body nodes, condensing all nodal degrees of freedom to only six; three for displacement and three for rotation. To form a linear set of equations to be solved, (2) is integrated in time with the Newmark method and is linearised about its primary variables (displacement of the background grid and motion of the rigid body).

### 3 Rigid Body interaction with Material Points

To model contact, the node-to-surface type formulation is applied here to the GIMPM [2, 3]. It is important to track any of the corners of the GIMP domains that interact with the rigid body, Figure 1, with contact determined using the closest point projection (CPP) method with the gap and gap vector functions,  $g^n$  and  $g_i^n$ ,

$$g_i^n(\xi^\alpha(\tau), \tau) = g^n(\xi^\alpha(\tau), \tau) n_i(\xi^\alpha(\tau), \tau) = x_i(\tau) - x_i'(\xi^\alpha(\tau), \tau) \quad \text{and} \quad g^n = g_i^n n_i. \quad (3)$$

Above,  $\tau$  is time,  $x_i$  is the GIMP domain's corner position,  $x_i'$  is the projected position onto the rigid body and  $\xi^\alpha$ , with  $\alpha \in [1, 2]$ , is the local coordinate of the triangular element  $\partial K$  that the GIMP corner is in contact with, shown in red in Figure 1. The derivative of  $g_i^n$  with respect to time gives the normal  $\dot{g}_i^n$  and a relative tangential velocity,  $\dot{g}_i^t$ , which enables a description of the movement of a particle along the rigid body,

$$\dot{g}_i^t = \int_T \dot{g}_i^t dt = \int_T \dot{g}_i^{slip} dt + \int_T \dot{g}_i^{stick} dt = \dot{g}_i^{slip} + \dot{g}_i^{stick}. \quad (4)$$

Using the above definitions, and following the work of [3], the contact residual can now be written as

$$\{R_c\} = \int_{\partial K \in \partial\mathcal{T}_c} (\delta g^n n_i p_i^n + \delta \xi^\alpha p_\alpha^t) dx = 0 \quad (5)$$

where  $\delta g^n$  and  $\delta \xi^\alpha$  are first variations provided in [3],  $p_i^n$  and  $p_\alpha^t$  are respectively the normal and tangential point forces, with  $(\cdot)^\alpha$  and  $(\cdot)_\alpha$  respectively defining the contravariant and covariant variables. The covariant form of the tangential force is  $p_\alpha^t = p_i^t (\partial x'_i / \partial \xi^\alpha)$  where  $p_i^t$  is a Cartesian vector of the frictional force and  $\varepsilon_n$  is the normal penalty, and  $p_i^n = \varepsilon_n g_i^n$  is the Cartesian form of the normal force.  $p_i^t$  is modelled using Coulomb stick-slip friction, it has two states, an elastic stick state and a dissipative slip state, respectively given as,

$$p_i^{stick} = \varepsilon_t g_i^{stick} \quad \text{and} \quad p_i^{slip} = \mu |p_n| \frac{\hat{g}_i^{slip}}{\|\hat{g}_i^{slip}\|} \quad \text{if} \quad \|p^{stick}\| > \mu |p_n| \quad (6)$$

where  $\mu |p^n|$  is the sticking force,  $\mu$  is a constant coefficient of friction and  $\varepsilon_t$  is the tangential penalty. The law is subject to the Karush-Kuhn-Tucker (KKT) conditions:  $f = \|p_i^{stick}\| - \mu p_n \leq 0$ ,  $\lambda \geq 0$  and  $f\lambda = 0$ , where  $f$  is a yield surface and  $\lambda$  is the rate of tangential slip. The state of contact is found using the trial elastic state provided in [2], if the elastic trial state is within the yield surface there is a stick condition, otherwise the contact points is slipping.

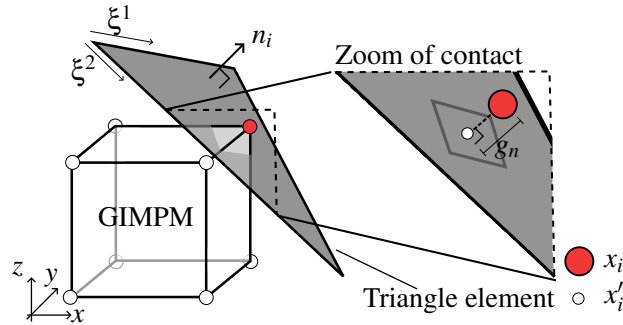


Figure 1: Diagram of the contact between a GIMP domain and a rigid body triangle.

#### 4 Numerical investigation

To validate the method, two problems are considered: a sphere rolling down an inclined slope to test the stick/slip contact [6], and an anchor is dragged through soil to demonstrate that the method is robust.

**3D Rolling sphere:** The results for this problem are provided in Figure 2a. The slope has dimensions  $W = L = 5\text{m}$  and the sphere a diameter  $d = 0.5\text{m}$ . The background element size,  $h = 0.25\text{ m}$ , with 8 GIMPs within each element. A time step of  $0.01\text{s}$  is used and to make the slope rigid all degrees of freedom are constrained. Three coefficients of friction are considered, at  $\mu = 0.0$  and  $0.2$  slip behaviour should occur, whilst at  $0.4$  it is a stick condition. The results in Figure 2a show very good agreement with the analytical result [6].

**Anchor:** The second problem is an anchor being dragged through a soil with a relative density of  $38\%$ , the material is modelled as linear elastic-plastic, the latter modelled with the Drucker-Prager model; both the anchor and soil are subject to gravity. This example demonstrates the method to be robust to a complex engineering scenario, and demonstrates the potential to model complicated geotechnical engineering problems. The anchor is being pulled at a velocity of  $0.5\text{ m/s}$ , the grid size is  $h = 0.2\text{ m}$  with 8 GIMPs per element and the time step is  $0.04\text{ s}$ . Figure 2b shows the anchor at load step 5 and Figure 2c at load step 100. Blue and red are respectively negative and positive vertical displacements.

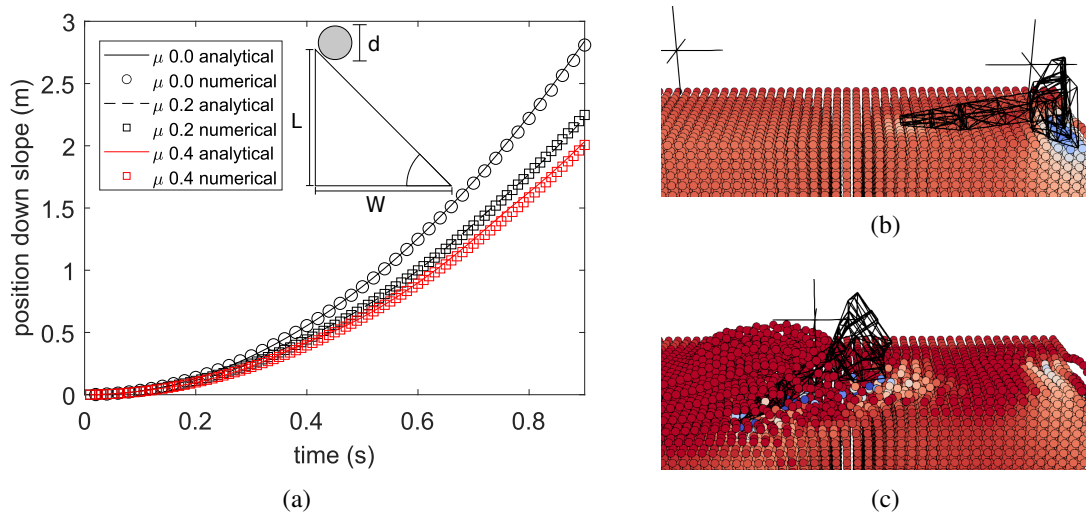


Figure 2: (a) shows a comparison of numerical and analytical results of a ball rolling down a hill, inset is the problem geometry. (b) and (c) show half an anchor being pulled through soil at load steps 5 and 100.

## 5 Conclusion

A GIMP for modelling contact with rigid bodies has been presented, it shows good agreement with analytical solutions and is able to model complicated geotechnical problems. The next step is to use the method to quantify the penetration of different anchor geometries in realistic soil conditions.

## Acknowledgements

This work was supported by the Engineering and Physical Sciences Research Council [grant numbers EP/W000970/1, EP/W000997/1 and EP/W000954/1].

## REFERENCES

- [1] Robinson, S., Brown, M.J., Matsui, H., Brennan, A., Augarde, C., Coombs, W. and Cortis, M. *A cone penetration test (CPT) approach to cable plough performance prediction based upon centrifuge model testing*, *Can. Geotech. J.*, (2021) **58**(10):1466-77.
- [2] Wriggers, P. *Computational contact mechanics*. Springer, Vol. 2., (2006).
- [3] Pietrzak, G., and Curnier, A. *Large deformation frictional contact mechanics: continuum formulation and augmented Lagrangian treatment*, *Comput. Methods Appl. Mech. Eng.*, (1999) **177**(3-4):351-381.
- [4] Charlton, T.J., Coombs, W.M., and Augarde, C.E. *iGIMP: An implicit generalised interpolation material point method for large deformations*, *Comput. Struct.*, (2017) **190**:108-125,
- [5] Coombs, W.M., and Augarde, C.E. *AMPLE: a material point learning environment*, *Adv. Eng. Softw.*, (2020) **139**:102748
- [6] Bardenhagen, S.G., Brackbill, J.U., and Sulsky, D., *The material-point method for granular materials*, *Comput. Methods Appl. Mech. Eng.*, (2000) **187**(3-4):529-541
- [7] Sharif, Y.U., Brown, M.J., Coombs, W.M., Augarde, C.E., Bird, R., Carter, G., MacDonald, C., & Johnson, K. (2023). *Characterization of Anchor Penetration Behaviour for Cable Burial Risk Assessment*. In *9th Int. SUT OSIG Conference "Innovative Geotechnologies for Energy Transition"*, London, September 12-14:555-562.